

# A Mechanical Model for Magnetized Relativistic Blastwaves

Shunke Ai<sup>1</sup><sup>\*</sup> and Bing Zhang<sup>1</sup><sup>†</sup>

<sup>1</sup>*Department of Physics and Astronomy, University of Nevada Las Vegas, Las Vegas, NV 89154, USA*

Accepted XXX. Received YYY; in original form ZZZ

## ABSTRACT

The evolution of a relativistic blastwave is usually delineated under the assumption of pressure balance between forward- and reverse-shocked regions. However, such a treatment usually violates the energy conservation law. A mechanical model of non-magnetized blastwaves was proposed in previous works to solve the problem. In this paper, we generalize the mechanical model to the case of a blastwave driven by an ejecta with an arbitrary magnetization parameter  $\sigma_{\text{ej}}$ . We test our modified mechanical model by considering a long-lasting magnetized ejecta and found that it is much better in terms of energy conservation than the pressure-balance treatment. For a constant luminosity  $L_{\text{ej}} = 10^{47} \text{ erg s}^{-1}$  and  $\sigma_{\text{ej}} < 10$ , the deviation from energy conservation is negligibly small at small radii, but only reaches less than 25% even at  $10^{19} \text{ cm}$  from the central engine. Assuming a finite lifetime of the central engine, the reverse shock crosses the magnetized ejecta earlier for the ejecta with a higher  $\sigma_{\text{ej}}$ . After shock crossing, all the ejecta energy is injected into the blastwave.

**Key words:** gamma-ray bursts – MHD – shock waves

## 1 INTRODUCTION

When a relativistic ejecta powered by a central engine interacts with an ambient medium, a forward shock (FS) would propagate into the medium and a reverse shock (RS) would propagate into the ejecta. The fluid between the FS and RS is defined as a blastwave. Usually, an FS/RS system is divided into four regions: (1) unshocked ambient medium; (2) shocked ambient medium; (3) shocked ejecta; (4) unshocked ejecta. A contact discontinuity separates region (2) from region (3) (Sari & Piran 1995; Zhang & Kobayashi 2005).

Such a blastwave system is very relevant to the early phase of gamma-ray burst (GRB) afterglow emission. Particles accelerated from both FS and RS contribute to the observed afterglow emission (Mészáros & Rees 1999; Sari & Piran 1999; Zhang et al. 2003; Kobayashi & Zhang 2003; Wu et al. 2003), see Gao et al. (2013) for a comprehensive discussion on all the possible spectral regimes and lightcurves from combined FS and RS emission. GRBs usually have a short duration so that the ejected shell has a finite thickness so that RS shock crossing occurs around the blastwave deceleration radius (Sari & Piran 1995; Zhang & Kobayashi 2005). In the case of the existence of a long-lived central engine, e.g. a rapidly spinning pulsar or magnetar (Dai & Lu 1998; Zhang & Mészáros 2001; Ai et al. 2018), continuous injection of Poynting-flux energy would be possible.

In the literature, a FS-RS blastwave system is usually treated assuming pressure balance, i.e.  $p_f = p_r$  where  $p_f$  and  $p_r$  are the

pressure in the forward-shocked-region (region (2)) and reverse-shocked-region (region (3)), respectively. The Lorentz factor across the blast wave is roughly a constant in space, which is verified through hydrodynamical simulation (Kobayashi & Sari 2000). Such a treatment gives a reasonable, approximate treatment of the problem (Sari & Piran 1995; Zhang & Kobayashi 2005). However, energy conservation is violated in such a treatment (Beloborodov & Uhm 2006; Yan et al. 2007; Uhm 2011). The reason is that pressure balance cannot be achieved immediately in a dynamically evolving system, and that there should exist a pressure gradient between the FS and RS. Beloborodov & Uhm (2006) proposed a mechanical model to treat the problem more precisely, which breaks the pressure balance in the blastwave. The model was studied by Uhm (2011) in detail, who demonstrated that energy conservation is preserved. In these treatments, a pure hydrodynamical (non-magnetized) blastwave was considered.

Observations and theoretical modeling of GRB early afterglow (e.g. Zhang et al. 2003; Troja et al. 2017) and prompt emission (e.g. Zhang & Yan 2011; Yonetoku et al. 2011; Uhm & Zhang 2014) suggest that at least for some GRBs, the ejecta is magnetically dominated (see (Kumar & Zhang 2015) for a review). It is therefore interesting to study the RS dynamics for an arbitrarily magnetized relativistic outflow. A detailed treatment of this problem was presented in Zhang & Kobayashi (2005) under the assumption of pressure balance (see also Fan et al. (2004) for the case of  $\sigma < 1$ ). Denoting the magnetization parameter of the ejecta as  $\sigma_{\text{ej}} = B^2/(4\pi\rho c^2)$ , where  $B$  is the magnetic field strength and  $\rho$  is the mass density, both in the co-moving frame of the fluid. The pressure balance condition states  $p_r + p_{r,b} = p_f$ , where  $p_f$  and  $p_r$  are the gas pressures in the forward- and reverse-shocked re-

\* E-mail: ais1@unlv.nv.edu

† E-mail: zhang@physics.unlv.edu

gions, respectively, and  $p_{r,b}$  is the magnetic pressure in the reverse-shocked region. Making use of the relativistic MHD shock jump condition (Kennel & Coroniti 1984; Zhang & Kobayashi 2005), one can treat the evolution of the blastwave in detail. A criteria  $\sigma_{ej} < 8/3\gamma_4^2(n_1/n_4)$  for the formation of an RS was proposed based on the pressure balance assumption (Zhang & Kobayashi 2005), where  $n_1$  and  $n_4$  are the number densities in regions (1) and (4), respectively, and  $\gamma_4$  is the bulk Lorentz factor of the ejecta (Zhang & Kobayashi 2005). Such a treatment can roughly delineate the magnetized blastwave, especially when the central engine duration is short. However, the energy conservation condition is not satisfied, and the deviation becomes significant if the central engine powers a long-lasting magnetized wind. To treat such a problem, a mechanical model is desirable, but such a model does not exist in the literature for an arbitrarily magnetized outflow.

In our work, we generalize the blastwave mechanical model to the regime for an ejecta with an arbitrary  $\sigma_{ej}$ . In section 2, we review the basic criteria to excite a magnetized relativistic shock, the shock jump conditions and their solutions. In section 3, we derive the governing equations for the evolution of a magnetized blastwave in a mechanical model. In section 4, we present the results of a long-lived neutron star as the central engine as an example and test the energy conservation criterion. Conclusions are presented in section 5 with some discussion.

## 2 MAGNETIZED RELATIVISTIC SHOCKS

In order to excite a shock in a relativistic hydrodynamic fluid, the relative speed between the two fluids should exceed the sound speed in the upstream, which reads (e.g. Zhang 2018) where  $c$  is the speed of light,  $\hat{\gamma}$  is the adiabatic index, which may be expressed as a function of the average internal Lorentz factor of the fluid (Kumar & Granot 2003; Uhm 2011),

$$\hat{\gamma} = \frac{4\bar{\gamma} + 1}{3\bar{\gamma}}. \quad (1)$$

For a magnetized fluid, one can define the magnetization parameter

$$\sigma = \frac{B_0^2}{4\pi\rho_0 c^2}, \quad (2)$$

where both  $B_0$  and  $\rho_0$  are the quantities in the comoving frame of the fluid. To excite a MHD shock in a magnetized ejecta, the relative speeds of two fluids must exceed the maximum speed of the fast magneto-acoustic (MA) wave in the upstream, which reads (e.g. Zhang 2018)

$$\begin{aligned} v_{F,\max} &= \sqrt{v_A^2 + c_s^2 \left(1 - \frac{v_A^2}{c^2}\right)} \\ &= c \sqrt{\frac{\hat{\gamma}p + \frac{B_0^2}{4\pi}}{\rho_0 c^2 + \frac{\hat{\gamma}}{\hat{\gamma}-1}p + \frac{B_0^2}{4\pi}}} \end{aligned} \quad (3)$$

For a highly magnetized cold upstream, i.e.  $\sigma \gg 1$  and  $p \ll \rho_0 c^2$ , the maximum speed of fast MA wave could be simplified and its corresponding Lorentz factor is

$$\gamma_{F,\max} = \sqrt{1 + \sigma}. \quad (4)$$

Once a shock is excited, the physical quantities in the upstream and downstream near the shock front are connected through the shock jump conditions. If the magnetic field lines are in the

shock plane, the shock jump condition for a magnetized fluid reads (Kennel & Coroniti 1984; Zhang & Kobayashi 2005)

$$n_1 u_{1s} = n_2 u_{2s} \quad (5)$$

$$E_s = \beta_{1s} B_{1s} = \beta_{2s} B_{2s} \quad (6)$$

$$\gamma_{1s} \mu_1 + \frac{E_s B_{1s}}{4\pi n_1 u_{1s}} = \gamma_{2s} \mu_2 + \frac{E_s B_{2s}}{4\pi n_2 u_{2s}} \quad (7)$$

$$\mu_1 u_{1s} + \frac{p_1}{n_1 u_{1s}} + \frac{B_{1s}^2}{8\pi n_1 u_{1s}} = \mu_2 u_{2s} + \frac{p_2}{n_2 u_{2s}} + \frac{B_{2s}^2}{8\pi n_2 u_{2s}}, \quad (8)$$

where  $n$  represents the particles' number density,  $u = \gamma\beta$  is the four velocity in the direction of fluid's motion,

$$\mu = \frac{h}{n} = m_p c^2 + e + p = m_p c^2 + \frac{\hat{\gamma} p}{\hat{\gamma} - 1} \quad (9)$$

is the specific enthalpy,  $e$  is the internal energy density, and  $p = (\hat{\gamma} - 1)e$  is the thermal pressure. Here we adopt the convention that a quantity  $Q_{ij}$  is defined as the value in region  $i$  in the rest frame of  $j$  and that the subscripts "1" and "2" represent the upstream and downstream, respectively, and the subscript "s" represents the shock. A quantity with only one subscript is defined in the rest frame of itself. With the "cold upstream" assumption, we have  $p_1 = e_1 = 0$  and  $\mu_1 = m_p c^2$ . Notice that one has one additional jump condition for MHD shocks (Equation 6) compared to the pure hydrodynamic shocks due to the continuity of the parallel electric field<sup>1</sup>.

Noting  $B_{is} = B_i \gamma_{is}$  ( $i = 1, 2$ ), using Equation 2 one can express the magnetized parameter in the upstream as

$$\sigma_1 = \frac{B_1^2}{4\pi\rho_1 c^2} = \frac{B_{1s}^2}{4\pi n_1 \mu_1 \gamma_{1s}^2}. \quad (10)$$

Combining the jump conditions with Equations 9 and 10, for a known  $n_1$ , all the quantities in the downstream can be expressed as a functions of  $u_{2s}$ ,  $\sigma_1$  and  $\gamma_{21}$  (Zhang & Kobayashi 2005)<sup>2</sup>:

$$u_{1s} = u_{2s}(\gamma_{21} \sigma_1 \gamma_{21} + [u_{2s}(\gamma_{21}, \sigma_1)^2 + 1]^{1/2}(\gamma_{21}^2 - 1)^{1/2}), \quad (11)$$

$$\frac{n_2}{n_1} = \frac{u_{1s}}{u_{2s}} \quad (12)$$

$$\frac{e_2}{n_2 m_p c^2} = (\gamma_{21} - 1) \left[1 - \frac{\gamma_{21} + 1}{2u_{1s} u_{2s}} \sigma_1\right] \quad (13)$$

$$\frac{B_2}{B_1} = \frac{u_{1s}}{u_{2s}}. \quad (14)$$

Here  $u_{2s}$  is calculated by solving a third-order equation derived from the jump conditions. Define  $x = u_{2s}^2$ , the equation reads (Zhang & Kobayashi 2005)

$$Jx^3 + Kx^2 + Lx + M = 0, \quad (15)$$

<sup>1</sup> Even though there is no electric field in the comoving frames of both upstream and downstream, the the rest frame of the shock (which moves relatively with respect to both streams), an electric field parallel to the shock front surface is induced due to Lorentz transformation, which is continuous across the shock. 6 is derived under the assumption that the plasma can be treated as a perfect conductor.

<sup>2</sup> Under the pressure balance assumption for blastwaves, magnetic pressure  $p_{b,i} = B_i^2/8\pi$  rather the strength of magnetic field was used in previous analyses. Here we consider  $B_i$  directly for the convenience of deriving the mechanical model later.

where

$$J = \hat{\gamma}(2 - \hat{\gamma})(\gamma_{21} - 1) + 2, \quad (16)$$

$$K = -(\gamma_{21} + 1)[(2 - \hat{\gamma})(\hat{\gamma}\gamma_{21}^2 + 1) + \hat{\gamma}(\hat{\gamma} - 1)\gamma_{21}]\sigma_1 \\ - (\gamma_{21} - 1)[\hat{\gamma}(2 - \gamma)(\gamma_{21}^2 - 2) + (2\gamma_{21} + 3)] \quad (17)$$

$$L = (\gamma_{21} + 1)[\hat{\gamma}(1 - \frac{\hat{\gamma}}{4})(\gamma_{21}^2 - 1) + 1]\sigma_1^2 \\ + (\gamma_{21}^2 - 1)[2\gamma_{21} - (2 - \hat{\gamma})(\hat{\gamma}\gamma_{21} - 1)]\sigma_1 \\ + (\gamma_{21} - 1)(\gamma_{21} - 1)^2(\hat{\gamma} - 1)^2 \quad (18)$$

$$M = -(\gamma_{21} - 1)(\gamma_{21} + 1)^2(2 - \hat{\gamma})^2\frac{\sigma_1^2}{4}, \quad (19)$$

with  $\hat{\gamma} = (4\gamma_{21} + 1)/(3\gamma_{21})$ . Equation 15 can be solved numerically with a given  $\sigma_1$  and  $\gamma_{21}$ . All the other quantities in the downstream right behind the shock front can be then calculated.

### 3 A MECHANICAL MODEL FOR MAGNETIZED BLASTWAVES

#### 3.1 Ideal MHD equations

Consider a magnetized FS-RS system which contains four regions. Instead of assuming pressure balance in the central two regions, we apply ideal MHD equations to describe the evolution of each fluid element. We have

$$\nabla_\mu(\rho u^\mu) = 0 \quad (20)$$

for mass conservation and

$$\nabla_\mu T^{\mu\nu} = 0 \quad (21)$$

for energy-momentum conservation, where  $\rho$  is the mass density of the blastwave in its comoving frame,  $\mu_u$  is the normalized 4-velocity of the blast wave, and  $T^{\mu\nu}$  is the energy-momentum tensor. For a magnetized blastwave, the energy-momentum tensor includes both fluid and electromagnetic components, i.e.

$$T^{\mu\nu} = T_{\text{FL}}^{\mu\nu} + T_{\text{EM}}^{\mu\nu}, \quad (22)$$

where

$$T_{\text{FL}}^{\mu\nu} = (\rho c^2 + e + p)u^\mu u^\nu + p\eta^{\mu\nu}, \quad (23)$$

and

$$T^{\mu\nu} = \frac{1}{4\pi}(F^\mu_\lambda F^{\lambda\nu} - \frac{1}{4}\eta^{\mu\nu} F^{\lambda\delta} F_{\lambda\delta}). \quad (24)$$

Here  $e$  and  $p$  stand for the internal energy and thermal pressure, and  $F^{\mu\nu}$  is the electromagnetic tensor.

Explicitly splitting equation 20 and 21 in 3+1 space-time, the dynamic of blastwave can be delineated by the following ideal MHD equations (e.g. Zhang 2018):

$$\frac{\partial(\gamma\rho)}{\partial t} + \nabla \cdot (\gamma\rho\mathbf{v}) = 0, \quad (25)$$

$$\frac{\partial}{\partial t}(\frac{\gamma^2 h}{c^2}\mathbf{v} + \frac{\mathbf{E}_L \times \mathbf{B}_L}{4\pi c}) + \nabla \cdot [\frac{\gamma^2 h}{c^2}\mathbf{v} \otimes \mathbf{v} + (p + \frac{E_L^2 + B_L^2}{8\pi})\mathbf{I} \\ - \frac{\mathbf{E}_L \otimes \mathbf{E}_L + \mathbf{B}_L \otimes \mathbf{B}_L}{4\pi}] = 0, \quad (26)$$

$$\frac{\partial}{\partial t}(\gamma^2 h - p - \gamma\rho c^2 + \frac{B_L^2 + E_L^2}{8\pi}) \\ + \nabla \cdot [(\gamma^2 h - \gamma\rho c^2)\mathbf{v} + \frac{c}{4\pi}\mathbf{E}_L \times \mathbf{B}_L] = 0. \quad (27)$$

Here  $B_L$ ,  $E_L$  and  $\mathbf{v}$  are the quantities defined in the lab frame, while others are in the rest frame of the fluid. Considering that the plasma in the blastwave can be treated as a perfect conductor, one can derive strength of electric field as

$$\mathbf{E}_L = -\frac{\mathbf{v}}{c} \times \mathbf{B}_L = -\boldsymbol{\beta} \times \mathbf{B}_L. \quad (28)$$

#### 3.2 Governing equation for the evolution of blastwaves

Since astrophysical blastwaves are usually powered by point-source central engine, we consider spherical geometry  $(r, \theta, \phi)$  throughout the paper. Since the ambient medium is usually not highly magnetized, we consider the interaction between a magnetized ejecta and a non-magnetized central engine.

To simplify the ideal MHD equations, we assume that the magnetic field lines in region 4 are in the  $\phi$  direction, which is parallel to the shock plane. Shock jump conditions dictate that the magnetic field lines in region 3 have the same direction as that in region 4. The bulk motion direction of the blastwave is the in the radial direction, i.e.  $\mathbf{v} = v\mathbf{e}_r$  so the electric field direction in the blastwave as viewed in the lab frame is in  $\theta$  direction, i.e.  $\mathbf{E}_L = E_L\mathbf{e}_\theta = \beta B_L\mathbf{e}_\theta$ . Therefore, we have

$$\mathbf{E}_L \times \mathbf{B}_L = \beta B_L^2 \mathbf{e}_r, \quad (29)$$

$$\mathbf{E}_L \otimes \mathbf{E}_L = \begin{bmatrix} 0 & 0 & 0 \\ 0 & E_L^2 & 0 \\ 0 & 0 & 0 \end{bmatrix} = \begin{bmatrix} 0 & 0 & 0 \\ 0 & \beta^2 B_L^2 & 0 \\ 0 & 0 & 0 \end{bmatrix} \quad (30)$$

and

$$\mathbf{B}_L \otimes \mathbf{B}_L = \begin{bmatrix} 0 & 0 & 0 \\ 0 & 0 & 0 \\ 0 & 0 & B_L^2 \end{bmatrix}. \quad (31)$$

With  $B_L = \gamma B$  (where  $B$  is the magnetic field of blastwave in its rest frame), Equation 26 and 27 can be simplified as

$$\frac{1}{c} \frac{\partial}{\partial t}(\gamma^2 h\beta) + \frac{1}{4\pi c} \frac{\partial}{\partial t}(\gamma^2 \beta B^2) + \frac{1}{r^2} \frac{\partial}{\partial r}(r^2 \gamma^2 h\beta^2) + \frac{\partial p}{\partial r} \\ + \frac{(1 + \beta^2)}{8\pi} \frac{\partial}{\partial r}(\gamma^2 B^2) + \frac{1}{4\pi r} (1 + \beta^2)\gamma^2 B^2 = 0 \quad (32)$$

and

$$\frac{\partial}{\partial t}(\gamma^2 h) - \frac{\partial}{\partial t}p + \frac{1}{8\pi} \frac{\partial}{\partial t}[(1 + \beta^2)\gamma^2 B^2] \\ + \frac{1}{r^2} \frac{\partial}{\partial r}(r^2 \gamma^2 h\beta c) + \frac{c}{4\pi r^2} \frac{\partial}{\partial r}(r^2 \beta \gamma^2 B^2) = 0. \quad (33)$$

Instead of investigating the profiles of various quantities in the blastwave, we define some integrated variables:

$$\Sigma = \int_{r_r}^{r_f} \rho dr, \quad (34)$$

$$P = \int_{r_r}^{r_f} p dr, \quad (35)$$

$$H = \int_{r_r}^{r_f} h dr, \quad (36)$$

$$\mathcal{B} = \int_{r_r}^{r_f} B^2 dr, \quad (37)$$

where  $r_r$  and  $r_f$  represent the distances of RS and FS from the central engine. Notice that the first three integrals were defined in the original mechanical model (Beloborodov & Uhm 2006; Uhm 2011). Also, we keep the assumption a constant velocity in the blastwave so that  $\frac{\partial \beta}{\partial r} = 0$ . Notice an identity for any function  $f(t, r)$

$$\int_{r_r(t)}^{r_f(t)} \frac{\partial}{\partial t} f(t, r) dr = \frac{d}{dt} \left[ \int_{r_r}^{r_f} f(t, r) dr \right] \\ + c[f_r \beta_r - f_f \beta_f], \quad (38)$$

where  $f_r$  and  $f_f$  are the values of  $f$  right behind the RS and FS in the rest frame of the blastwave, respectively, and  $\beta_r$  and  $\beta_f$  are the

velocities of RS and RS in the lab frame, respectively. One can then integrate Equations 25, 32, and 33. Define the distance of the contact discontinuity from the central engine as  $r_d$  and the dimensionless speed of the contact continuity as  $\beta$ , one then has  $\frac{d}{dt} = \beta c \frac{d}{dr_d}$ . The three equations can be then expressed as<sup>3</sup>

$$\frac{\beta}{r_d^2} \frac{d}{dr_d} (r^2 \Sigma \Gamma) = \Gamma [\rho_r (\beta - \beta_r) + \rho_f (\beta_f - \beta)] \quad (39)$$

$$\begin{aligned} & \frac{\beta}{r_d^2} \frac{d}{dr_d} (r^2 \Gamma^2 H \beta) - \Gamma^2 \beta [h_r (\beta - \beta_r) + h_f (\beta_f - \beta)] \\ & + \frac{\beta}{4\pi} \frac{d}{dr_d} (\Gamma^2 \beta \mathcal{B}) + \frac{\beta \Gamma^2}{4\pi} [B_r^2 \beta_r - B_f^2 \beta_f] + (p_f - p_r) \\ & + \frac{\Gamma^2 (1 + \beta^2)}{8\pi} (B_f^2 - B_r^2) + \frac{(1 + \beta^2) \Gamma^2 \mathcal{B}}{4\pi r_d} = 0 \end{aligned} \quad (40)$$

$$\begin{aligned} & \frac{\beta}{r^2} \frac{d}{dr_d} (r^2 \Gamma^2 H) - \Gamma^2 [h_r (\beta - \beta_r) + h_f (\beta_f - \beta)] \\ & - \beta \frac{dP}{dr_d} - (\beta_r p_r - \beta_f p_f) + \frac{\beta}{8\pi} \frac{d}{dr_d} [(1 + \beta^2) \Gamma^2 \mathcal{B}] \\ & + \frac{(1 + \beta^2) \Gamma^2}{8\pi} (\beta_r B_r^2 - \beta_f B_f^2) + \frac{\Gamma^2 \beta}{4\pi} (B_f^2 - B_r^2) \\ & + \frac{\beta \Gamma^2 \mathcal{B}}{2\pi r_d} = 0 \end{aligned} \quad (41)$$

Here,  $\Gamma = \gamma$ , which is used to keep consistency with the format of other variables. Since  $\frac{d\beta}{dr_d} = \frac{1}{\beta \gamma^2} \frac{d\gamma}{dr_d}$ , we totally have 5 independent unknowns ( $\Gamma, \Sigma, P, H, \mathcal{B}$ ). Besides Equations 39 - 41, one needs two more equations to close the problem. The first one is equation of state of fluid, which reads (e.g. Beloborodov & Uhm 2006; Uhm 2011).

$$H = \Sigma c^2 + \frac{\hat{\gamma}}{\hat{\gamma} - 1} P. \quad (42)$$

Another equation comes from the accumulation of integrated magnetic fields. Practically, it is easier to calculate an integral over volume than over radius. Define  $\mathcal{B}_{\text{sph}} = \int B^2 dV$ , where  $dV = dV'/\Gamma$  is the incremental volume at the RS in the lab frame and  $dV'$  is that in the comoving frame. The incremental particle number at the RS front is  $dN = \rho_r dV'/m_p$ , which is defined by the properties of the injected wind by

$$dN = \frac{dE_{\text{inj,p}}}{\gamma_4 m_p c^2}, \quad (43)$$

where  $dE_{\text{inj,p}}$  is the injected particle energy during lab-frame time  $dt$  into the RS. Assuming that the magnetization parameter in each  $dN$  shell is uniform, one can express the magnetization parameter at the RS downstream as

$$\sigma_r = \frac{B_r^2 dV}{4\pi \rho_r c^2 (dV'/\Gamma)} = \frac{d\mathcal{B}_{\text{sph}}}{4\pi m_p c^2 (dN/\Gamma)}. \quad (44)$$

For a low- $\sigma$  relativistic blastwave,  $r_r$  and  $r_f$  are very close so that one may adopt the approximation  $r_r \approx r_f \approx r_d$ . However, in the high  $\sigma$  regime, the RS velocity in the lab frame,  $\beta_r$ , is significantly

smaller than the FS velocity in the lab frame,  $\beta_f$ . Under certain conditions, the RS could even move back towards the central engine. The  $r_r \approx r_f \approx r_d$  approximation is no longer valid. Since  $B$  may change much more drastically near the RS than anywhere else, the relation between  $\mathcal{B}$  and  $\mathcal{B}_{\text{sph}}$  evolution may be found from

$$\begin{aligned} \frac{d\mathcal{B}_{\text{sph}}}{dt} &= \frac{d}{dt} \left[ \int_{r_r}^{r_f} 4\pi r^2 B^2 dr \right] \\ &= \int_{r_r}^{r_f} \frac{d}{dt} (4\pi r^2 B^2) dr + 4\pi r_r^2 B_r^2 (\beta - \beta_r) c \\ &\approx 4\pi r_r^2 \frac{d\mathcal{B}}{dt} + 8\pi r_d \mathcal{B} \beta c \end{aligned} \quad (45)$$

Rewriting Equation 45 in terms of  $dr_d$  instead of  $dt$ , one gets

$$\frac{d\mathcal{B}}{dr_d} = \frac{1}{4\pi r_r^2} \frac{d\mathcal{B}_{\text{sph}}}{dr_d} - 2\mathcal{B} \frac{r_d}{r_r^2}, \quad (46)$$

where  $d\mathcal{B}_{\text{sph}}$  can be obtained from Equations 43 and 44, once  $dE_{\text{inj}}$  is given. Now we have closed the problem. The evolution of blast wave is governed by Equations 39 - 41, 42 and 46.

#### 4 BLASTWAVE POWERED BY A LONG-LASTING MAGNETIZED EJECTA

We now apply the mechanical model to study the dynamics of a blastwave powered by a long-lasting magnetized ejecta with a constant magnetization parameter  $\sigma_{\text{ej}}$ . It interacts with an ambient medium to excite a FS - RS system under some conditions<sup>4</sup>. For simplicity, we assume a constant Lorentz factor ( $\gamma_{\text{ej}}$ ) for the ejecta. Then energy injected into the blast wave at each time interval can be calculated as

$$dE_{\text{inj}} = L_{\text{ej}} \frac{\beta_{\text{ej}} - \beta_r}{\beta_{\text{ej}}} dt = L_{\text{ej}} \frac{\beta_{\text{ej}} - \beta_r}{\beta_{\text{ej}}} \frac{dr_d}{\beta c}, \quad (47)$$

where  $L_{\text{ej}}$  is the luminosity of the central engine. The contribution from the particles' kinetic energy to the total injected energy is  $dE_{\text{inj,p}} = dE_{\text{inj}}/(1 + \sigma_{\text{ej}})$ , which is used to calculate  $dN$  in Equation 43.

With known  $L_{\text{ej}}$  and  $\sigma_{\text{ej}}$ , one can calculate the quantities in region 4 near the RS, including the number density

$$n_4 = \frac{L_{\text{ej}}}{4\pi r_r^2 \beta_{\text{ej}} \gamma_{\text{ej}}^2 c^3 m_p (1 + \sigma_{\text{ej}})} \quad (48)$$

and the magnetic field

$$B_4 = (4\pi n_4 m_p c^2 \sigma_{\text{ej}})^{1/2}. \quad (49)$$

Given an initial value of  $\Gamma$ , one can calculate the relative velocity between the bulk motion of the blastwave and the unshocked ejecta, which reads

$$\beta_{34} = \frac{\beta_{\text{ej}} - \beta}{1 - \beta \beta_{\text{ej}}}. \quad (50)$$

so that the corresponding Lorentz factor is  $\gamma_{34} = [1/(1 - \beta_{34}^2)]^{1/2}$ . Now we can solve Equation 15 to solve  $u_{3,rs}$  and then calculate  $\rho_r, p_r, h_r$  and  $B_r$ . Similarly, we have  $\gamma_{21} = \Gamma$  and obtain  $\rho_f, p_f, h_f$  and  $B_f$ . Note that  $B_f = 0$  is satisfied for non-magnetized ISM.

<sup>3</sup> Notice that we do not consider the profiles of the quantities in the blastwave. Rather, we approximate the defined integrated quantities as the properties of a point-like fluid at contact discontinuity  $r_d$ , i.e.  $f(r) = F\delta(r - r_d)$ , where  $F$  stands for any of the integrated quantities defined in Equations 34 - 37. However, there should be no time derivative involved in the terms with this approximation.

<sup>4</sup> The criteria  $\sigma_{\text{ej}} < (8/3)\gamma_4(n_1/n_4)$  proposed in Zhang & Kobayashi (2005) is a good approximation in most cases. In this paper, we only use the most fundamental criterion, which requires the relative speed of two fluids to be greater than the sound speed (or maximum speed of the fast MA wave) in the upstream fluid.

Substituting the values of the quantities at the forward and reverse shocks to the governing equations listed in 3.2, the evolution of the blastwave can be solved.

Figure 1 shows the calculated blastwave evolution in the mechanical model. For comparison, we also plot the evolution of the blast wave under the pressure balance assumption in the same figure. As one can see, there is an apparent difference between the pressure balance model and the mechanical model. It has been discussed in Uhm (2011) that once pressure balance was assumed, the expansion of the blastwave caused by  $pdV$  work would be ignored, which would lead to an underestimation of the blast wave's Lorentz factor  $\Gamma$ . In the magnetized blastwaves, the contribution of magnetic pressure is equivalent to thermal pressure. Hence,  $\Gamma$  is again underestimated for a magnetized fluid in the pressure-balance model.

We test the mechanical model from the view point of energy conservation. The total energy of the blastwave can be obtained by integrating the 00 component of the Energy-momentum tensor over the volume between the forward and reverse shocks, which is expressed as

$$E_{bw} = \int_{r_r}^{r_f} (\Gamma^2 h - p + \frac{\Gamma^2 B^2}{4\pi}) 4\pi r^2 dr \approx 4\pi r_d^2 (\Gamma^2 H - P + \frac{\Gamma^2 \mathcal{B}}{4\pi}). \quad (51)$$

With the pressure balance assumption, the profile of all the quantities should be uniform in region 2 and region 3, respectively. Therefore, the expression of total energy of the blastwave can be written as<sup>5</sup>

$$E_{bw} \approx 4\pi r_d^2 (\Gamma^2 h_r - p_r + \frac{\Gamma^2 B^2}{4\pi})(r_d - r_r) + 4\pi r_d^2 (\Gamma^2 h_f - p_f)(r_f - r_d). \quad (52)$$

However, both Equation 52 and the second line of Equation (51) are valid only when  $r_r \sim r_d \sim r_f$  is satisfied. For the mechanical model, it is convenient to calculate the energy of the blastwave directly through the volume integrals of the quantities, which can reduce the error introduced by spherical expansion. The blastwave energy in mechanical model reads

$$E_{bw,mech} = \Gamma^2 H_{sph} + P_{sph} + \frac{\Gamma^2 \mathcal{B}_{sph}}{4\pi}, \quad (53)$$

where the volume integrated quantities  $H_{sph} = \int_{r_r}^{r_f} 4\pi r^2 h dr$  and  $P_{sph} = \int_{r_r}^{r_f} 4\pi r^2 p dr$  can be derived from  $H$  and  $P$  with the similar relationship shown in Equation 46.

In principle, the total energy injected to the blastwave should be equal to the total energy of the blastwave plus the rest mass energy of the ambient medium being swept ( $E_{1,sw} = \frac{4\pi}{3} r_f^3 n_1 m_p$ ). Thus, the ratio between the two can be used for the energy conservation test. As we can see from the lower right panel of Figure 1, both models satisfy the energy conservation well in the early stage when  $r_r \sim r_f$ . However, the error increases quickly as the blastwave expands. If the energy of blast wave is calculated with Equation 51 and 52. For the pressure balance model, the deviation exceeds 25% within  $r_d = 10^{17}$ cm with a large  $\sigma_{ej}$  values. For mechanical model, on the other hand, the deviation could be always smaller than 10% within the distance  $r_d = 10^{18}$ cm for  $\sigma_{ej} < 10$ . If the energy of

blast wave is calculated with Equation 53, the deviation is negligible within  $r_d = 10^{17}$ cm and is smaller than 25% within  $r = 10^{19}$ cm for  $\sigma_{ej} < 10$ . All in all, the mechanical model satisfies the energy conservation much better than the pressure balance model.

In reality, the central engine timescale cannot be infinitely long. For example, a newly born neutron star with an initial spin period  $P_0 \sim 1$  ms and a fiducial value of moment of inertia  $I = 3 \times 10^{45}$ erg s<sup>2</sup> would have a total rotational energy  $E_{rot} = (1/2)I\Omega^2 \sim 10^{53}$ erg. Assuming that the magnetized ejecta is the wind of the NS with a luminosity of  $L_{ej} = 10^{47}$ erg s<sup>-1</sup>, one can obtain an upper limit of the central engine timescale as  $\tau < 10^6$ s. Since the strength of the poloidal magnetic field decreases with distance from the central NS as  $B_p \sim R^{-2}$  while that of the toroidal magnetic field decreases as  $B_d \sim R^{-1}$ , the magnetic field beyond the light cylinder would be dominated by the  $\phi$  component, which agrees with the geometry we discussed in section 3.2.

With a finite central engine timescale, the reverse shock would eventually cross the ejecta at some time. Rather than adopting the upper limit of the central engine timescale, here we choose a more realistic value  $\tau = 10^4$ s as an example<sup>6</sup>. Other parameters are the same as those adopted in Figure 1, thus the evolution history should be also the same. However, instead of always having a stable FS - RS system, there will be a RS crossing time, after which the blastwave would experience a relaxation process before entering the he Blandford-McKee regime (Blandford & McKee 1976). We stop our calculation at the RS crossing time, when essentially all the energy from the ejecta is injected into the blastwave. Since the rest mass energy of the ambient medium is negligible, the energy of the blastwave should always be the same at this time, regardless of the value of the magnetization parameter  $\sigma_{ej}$ .

The results are shown in Figure 2. As we can see, the energy of the blastwave at the RS crossing time is roughly  $E_{bw} \sim 10^{51}$ erg, which is consistent with the value estimated from  $E_{bw} \sim L_{ej}\tau$ . We also calculate the timescale of the blastwave evolution in the lab frame, which shows that the RS crosses the ejecta earlier for an ejecta with a higher  $\sigma_{ej}$ . This is understandable since shock propagates faster in the stronger magnetized upstream (Zhang & Kobayashi 2005).

## 5 CONCLUSION AND DISCUSSION

In this work, we extended the mechanical model for hydrodynamical blastwaves (Beloborodov & Uhm 2006; Uhm 2011) to the magnetically dominated regime and calculate the evolution of a blastwave driven by a magnetized ejecta. We break the pressure balance assumption ( $p_r = p_f$ ) and derive the governing equations of the evolution from the basic ideal MHD equations. The blastwave is treated as a whole, i.e. we consider only the integrated quantities of the blastwave rather than the fluid elements and their profiles within the blastwave. By defining four integrated quantities (Equations 34-37), we derive four governing equations (Equations 39 - 41, 42 and 46) to solve the blastwave problem. Through various tests, we find that the mechanical model is in general much better than the pressure balance model in terms of energy conservation, especially in the high  $\sigma_{ej}$  regime. For a central engine with an infinitely long central engine time, our mechanical model works precisely at small radii, and only deviates from energy conservation within 25%

<sup>5</sup> Equation 52 is equivalent to  $E_{bw} = \frac{4\pi}{3} (\Gamma^2 h_r - p_r + \frac{\Gamma^2 B_r^2}{4\pi})(r_d^3 - r_r^3) + \frac{4\pi}{3} (\Gamma^2 h_f - p_f)(r_f^3 - r_d^3)$ , when  $r_f \sim r_r \sim r_d$ . However, with the expansion of the blastwave, the latter equation would introduce an even larger error.

<sup>6</sup> For a rapidly spinning NS, there could be other mechanisms (such as secular gravitational waves, Fan et al. (2013); Gao et al. (2016)) to release the rotational energy.

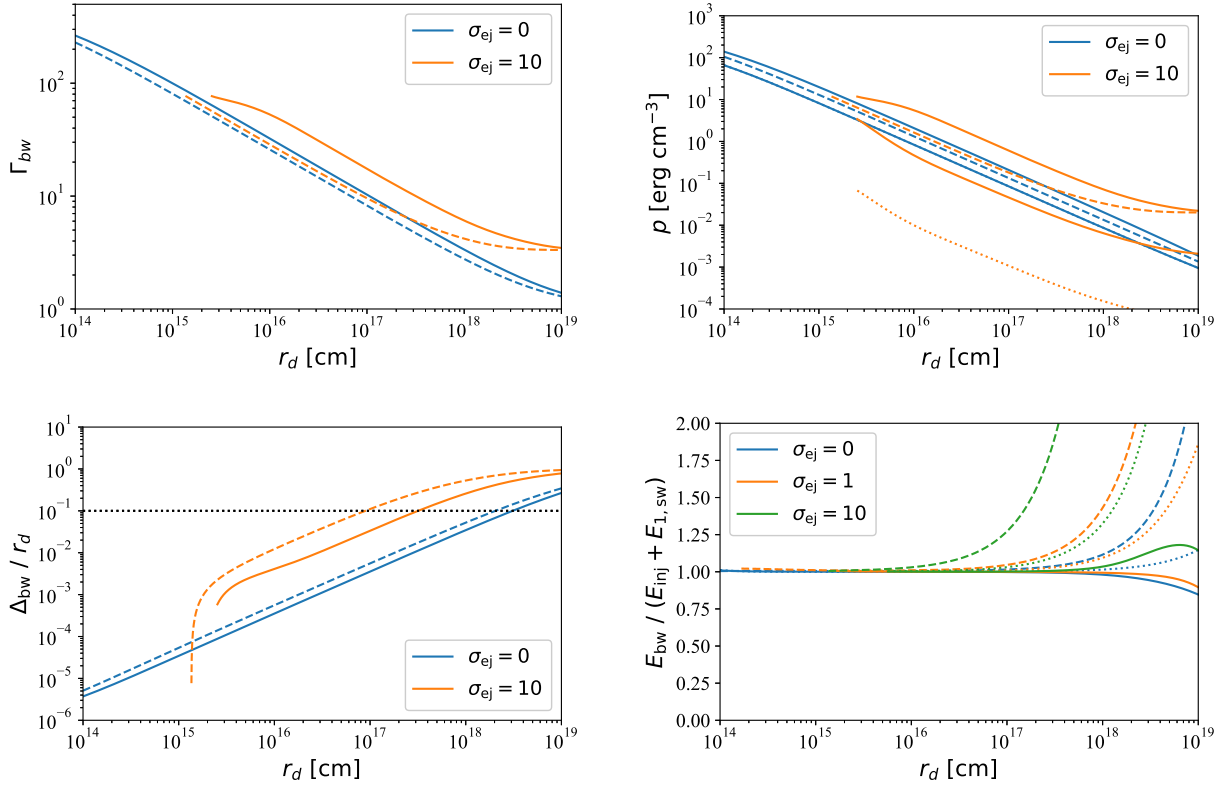


**Figure 1.** The evolution of the properties of the blast wave with  $L_{ej} = 10^{47} \text{ erg s}^{-1}$  and an infinite central engine lifetime.  $\gamma_{ej} = 500$  and  $n_1 = 1 \text{ cm}^{-3}$  are assumed. Different colors represent different values of the magnetization parameter  $\sigma_{ej}$ . Solid lines represent the mechanical model and dashed lines represent the pressure balance model. Upper left panel: the evolution of Lorentz factor of the blast wave; Upper right panel: the evolution of pressure. The solid lines above and below the dashed lines represent total pressure behind RS ( $p_{r,tot}$ ) and FS ( $p_f$ ) respectively. The dotted dashed line is the thermal pressure behind the reverse shock ( $p_r$ ) with  $\sigma_{ej} = 10$ . Lower left panel: the thickness of the blast wave normalized to the radius of contact discontinuity. The black dotted line represents the level where the thickness is an order of magnitude smaller than the radius of contact discontinuity. Lower right panel: The ratio between the blastwave's energy and the energy injected to the blastwave from the RS and FS. We calculate the energy of blastwave through Equation 52 for the pressure balance model (dashed lines) and Equation 53 for the mechanical model (solid lines). We also calculate the blastwave energy for the mechanical model with Equation 51 (dotted lines).

for  $\sigma_{ej} < 10$  at a distance  $r_d < 10^{19} \text{ cm}$  from the central engine. For more realistic cases with limited engine timescale  $\tau = 10^4 \text{ s}$ , we checked RS crossing timescales for different  $\sigma_{ej}$  values and reached expected results.

It is worth noticing that the pressure balance treatment is a nice approximation when calculating the evolution of a blastwave with a short engine time or a low  $\sigma_{ej}$ , so those treatments can give reasonable approximations for GRB FS-RS problems (Sari & Piran 1995; Zhang & Kobayashi 2005). However, a mechanical model is needed when dealing with blastwave problems with a long lasting central engine (e.g. Uhm et al. 2012), especially when the engine is highly magnetized. Our developed theory would be useful to treat problems invoking energy injection of a long-lived engine in various explosive events, especially for the possible pulsar-powered kilonova following neutron star mergers (e.g. Yu et al. 2013; Metzger & Piro 2014). This problem will be treated in detail using the mechanical model proposed in this paper in a future work.

Another approach of improving the pressure balance model to preserve energy conservation has been discussed in the literature (Yan et al. 2007; Chen & Liu 2021). The energy conservation requirement is imposed by hand, and the pressures are assumed to be uniform in regions 2 and 3 but discontinuous at the contact dis-

continuity. Such an ad hoc treatment can reach similar conclusion as ours (Chen & Liu 2021), but has larger deviations in the high  $\sigma$  regime.

## ACKNOWLEDGEMENTS

This work is supported by the Top Tier Doctoral Graduate Research Assistantship (TTDGRA) at University of Nevada, Las Vegas.

## REFERENCES

- Ai S., Gao H., Dai Z.-G., Wu X.-F., Li A., Zhang B., Li M.-Z., 2018, *ApJ*, **860**, 57
- Beloborodov A. M., Uhm Z. L., 2006, *ApJ*, **651**, L1
- Blandford R. D., McKee C. F., 1976, *Physics of Fluids*, **19**, 1130
- Chen Q., Liu X.-W., 2021, arXiv e-prints, p. arXiv:2104.00509
- Dai Z. G., Lu T., 1998, *A&A*, **333**, L87
- Fan Y. Z., Wei D. M., Wang C. F., 2004, *A&A*, **424**, 477
- Fan Y.-Z., Wu X.-F., Wei D.-M., 2013, *Phys. Rev. D*, **88**, 067304
- Gao H., Lei W.-H., Zou Y.-C., Wu X.-F., Zhang B., 2013, *New Astron. Rev.*, **57**, 141
- Gao H., Zhang B., Lü H.-J., 2016, *Phys. Rev. D*, **93**, 044605

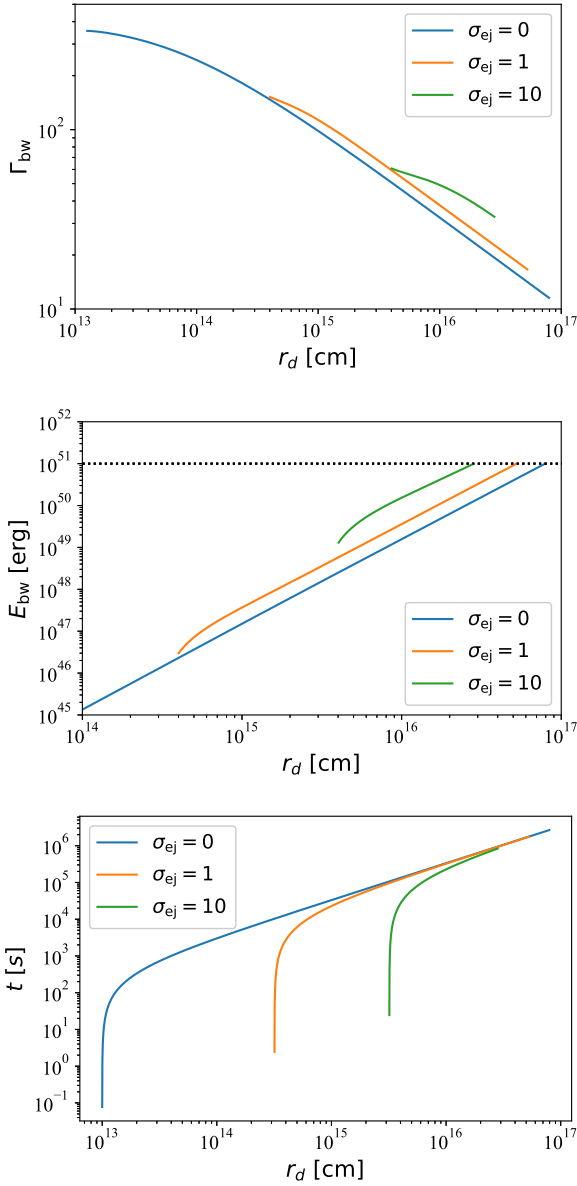


**Figure 2.** Blastwave evolution for a central engine with a finite timescale. Upper panel: the evolution of Lorentz factor. Middle panel: the evolution of blastwave energy. Lower panel: the timescale of the evolution of blastwave in the lab frame since the moment when a stable FS - RS system forms. the central engine duration  $\tau = 10^4 s$  is adopted for all the panels. Different colors represent different  $\sigma_{ej}$  values.

- Kennel C. F., Coroniti F. V., 1984, *ApJ*, 283, 694  
 Kobayashi S., Sari R., 2000, *ApJ*, 542, 819  
 Kobayashi S., Zhang B., 2003, *ApJ*, 597, 455  
 Kumar P., Granot J., 2003, *ApJ*, 591, 1075  
 Kumar P., Zhang B., 2015, *Phys. Rep.*, 561, 1  
 Mészáros P., Rees M. J., 1999, *MNRAS*, 306, L39  
 Metzger B. D., Piro A. L., 2014, *MNRAS*, 439, 3916  
 Sari R., Piran T., 1995, *ApJ*, 455, L143  
 Sari R., Piran T., 1999, *ApJ*, 520, 641  
 Troja E., et al., 2017, *Nature*, 551, 71  
 Uhm Z. L., 2011, *ApJ*, 733, 86  
 Uhm Z. L., Zhang B., 2014, *Nature Physics*, 10, 351  
 Uhm Z. L., Zhang B., Hascoët R., Daigne F., Mochkovitch R., Park I. H.,

2012, *ApJ*, 761, 147

Wu X. F., Dai Z. G., Huang Y. F., Lu T., 2003, *MNRAS*, 342, 1131

Yan T., Wei D.-M., Fan Y.-Z., 2007, *Chinese J. Astron. Astrophys.*, 7, 777

Yonetoku D., et al., 2011, *ApJ*, 743, L30

Yu Y.-W., Zhang B., Gao H., 2013, *ApJ*, 776, L40

Zhang B., 2018, The Physics of Gamma-Ray Bursts, doi:10.1017/9781139226530.

Zhang B., Kobayashi S., 2005, *ApJ*, 628, 315

Zhang B., Mészáros P., 2001, *ApJ*, 552, L35

Zhang B., Yan H., 2011, *ApJ*, 726, 90

Zhang B., Kobayashi S., Mészáros P., 2003, *ApJ*, 595, 950

This paper has been typeset from a  $\text{\LaTeX}$  file prepared by the author.